Supporting Information

Controllable synthesis of hierarchical $NiCo_2S_4$@Ni_3S_2 core-shell nanotube arrays with excellent electrochemical performance for aqueous asymmetric supercapacitors

Taobin He, Senlin Wang*, Fengxia Lu, Mucan Zhang, Xiao Zhang, Lin Xu

College of Materials Science & Engineering, Huaqiao University, Xiamen, Fujian, 361021, People's Republic of China

*Corresponding author. Fax: +86-595-22693746. *E-mail address:* slwang@hqu.edu.cn

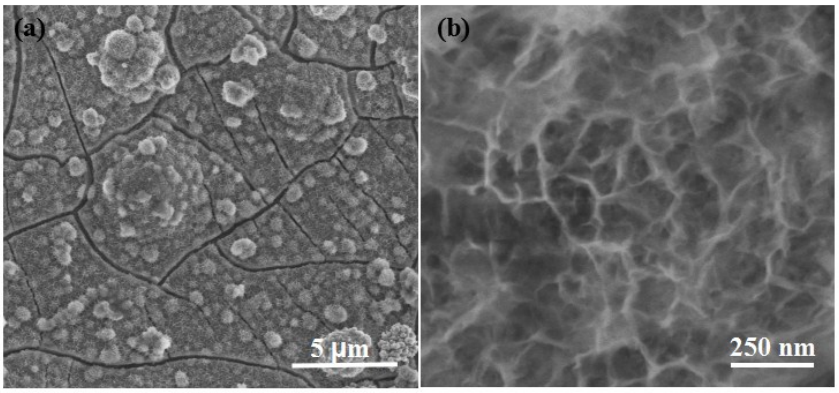

Fig. S1 (a) Low-magnification and (b) high-magnification FESEM images of Ni_3S_2 nanaosheets.

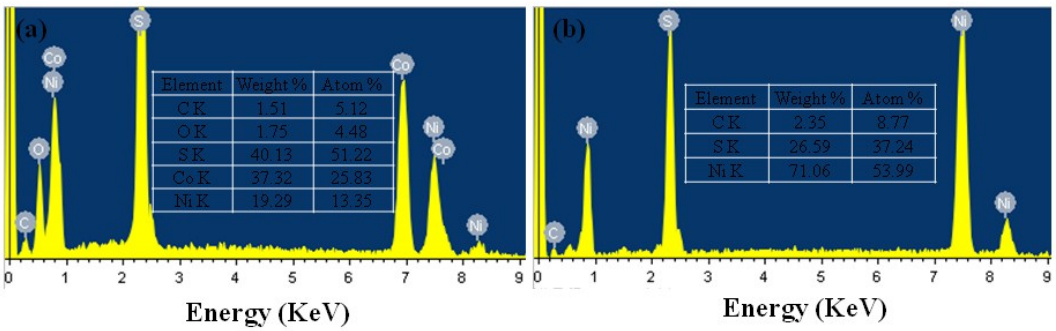

Fig. S2 EDS analysis of the $NiCo_2S_4$ NTAs (a) and the Ni_3S_2 nanosheets (b).

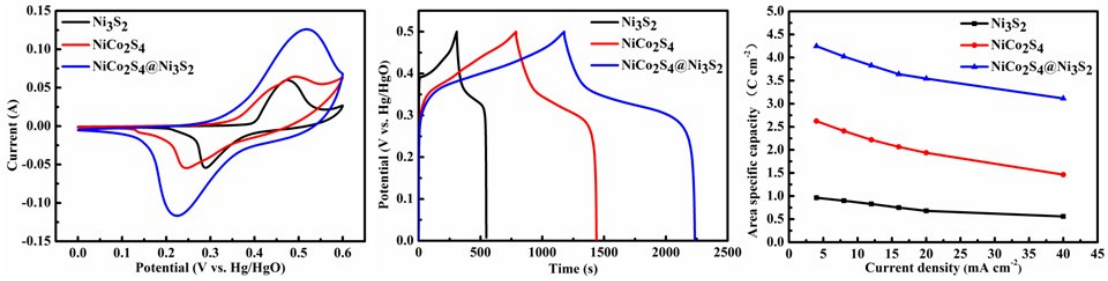

Fig. S3 the supercapacitor performance of Ni_3S_2 compared with $NiCo_2S_4$ and $NiCo_2S_4$@Ni_3S_2.

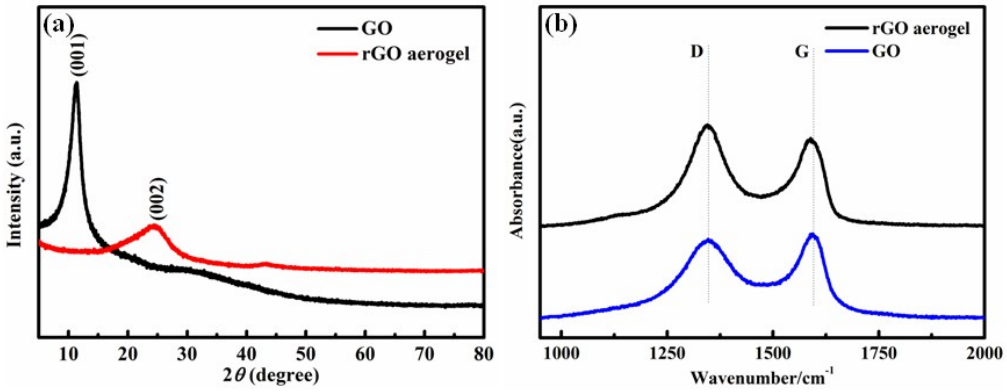

Fig. S4 (a) XRD patterns of GO and rGO aerogel, (b) The Raman spectra of the GO and rGO aerogel.

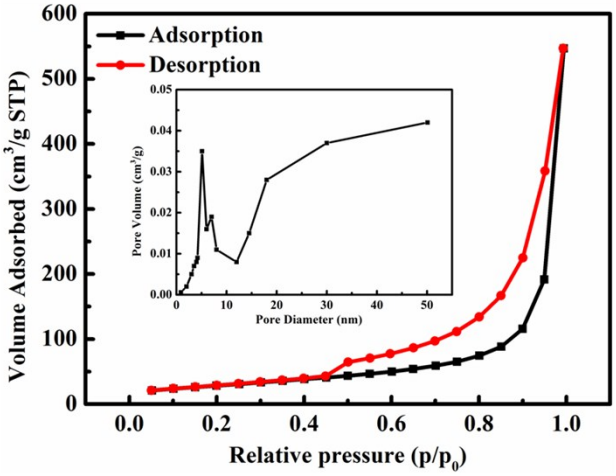

Fig. S5 N_2 adsorption–desorption isotherms of 3D rGO aerogel. The inset of Fig. S5 shows the corresponding BJH pore size distribution for 3D rGO aerogel.

Sample	BET Surface Area ($m^2 g^{-1}$)	Micropore Area ($m^2 g^{-1}$)	Total Pore Volume ($cm^3 g^{-1}$)	Micropore Volume ($cm^3 g^{-1}$)	Average Pore Diameter (nm)
3D rGO	168.6	19.4	0.56	0.008	9.6

Table S1. Specific surface areas and pore parameters of 3D rGO aerogel.

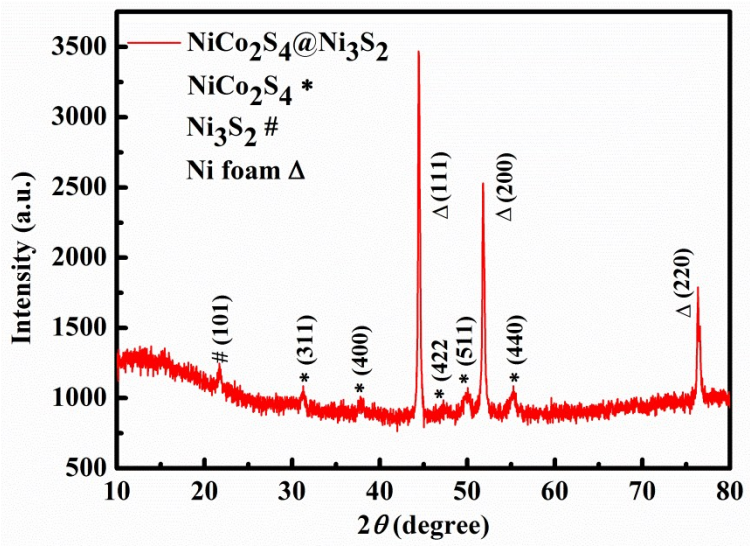

Fig. S6 The XRD pattern of $NiCo_2S_4@Ni_3S_2$ on the surface of the Ni foam after 5000 cycling test.

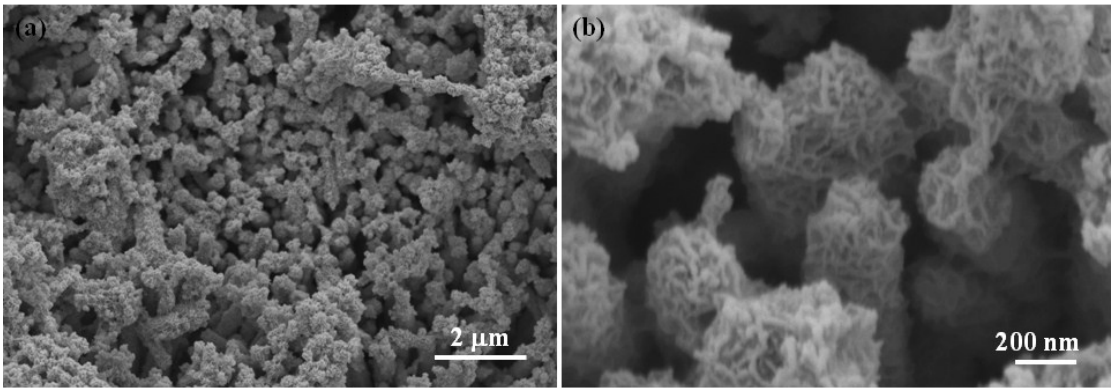

Fig. S7 The FESEM image of $NiCo_2S_4@Ni_3S_2$ on the surface of the Ni foam after 5000 cycling test.

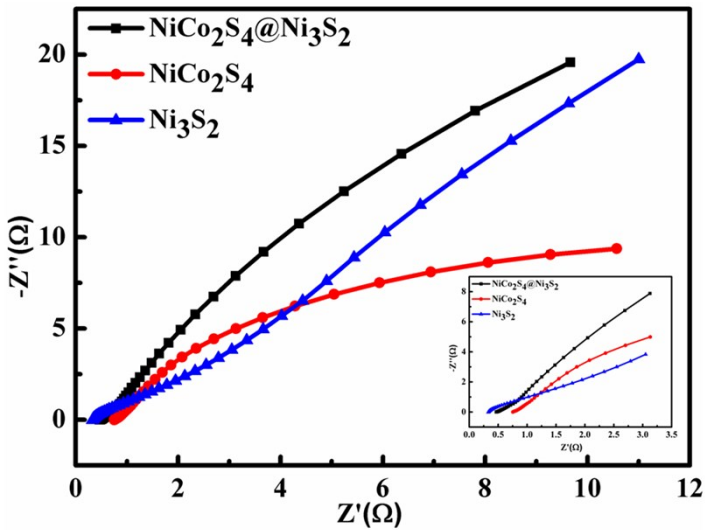

Fig. S8 Nyquist plots of $NiCo_2S_4$ and $NiCo_2S_4$@Ni_3S_2 and Ni_3S_2.